ELSEVIER

Catalysis Today 49 (1999) 401–409

CATALYSIS TODAY

Measurement of interatomic connectivities in molecular sieves using MQMAS-based methods

M. Pruski[a,*], C. Fernandez[b], D.P. Lang[a], J.-P. Amoureux[b]

[a]*Ames Laboratory, Iowa State University, Ames, IA 50011, USA*
[b]*Université de Lille, LDSMM, F-59655, Villeneuve d'Ascq, France*

Abstract

The multiple-quantum magic angle spinning (MQMAS) NMR method can be extended to allow for investigation of the interatomic connectivities between quadrupolar and spin-$\frac{1}{2}$ nuclei. Several new experiments will be reviewed that combine MQMAS with cross polarization (CP) or heteronuclear recoupling via rotational echo double resonance (REDOR) in order to probe the dipolar interactions between quadrupolar and spin-$\frac{1}{2}$ nuclei under high-resolution conditions. The theoretical and experimental aspects of the spin dynamics involved in these new methods will be discussed. Examples of experimental results will be presented, involving the ^{1}H–^{27}Al , and ^{19}F–^{27}Al spin pairs in fluorinated and hydrated aluminophosphates. © 1999 Elsevier Science B.V. All rights reserved.

1. Introduction

Enormous progress has been made during the last decade in developing methods to overcome anisotropic line broadening in the NMR spectra of half-integer quadrupolar spins in solids [1–4]. This broadening arises mainly from the coupling of the nonspherical charge distribution of such nuclei with the gradient of the electric field created by the surrounding electrons. It is usually much stronger and 'more anisotropic' than the chemical shift anisotropy (CSA) and dipolar effects. Due to the presence of significant higher order orientational terms, the complete averaging of second order quadrupolar broadening requires more complex motions of the sample, or the spin magnetization. Line narrowing via mechanical means was achieved using double rotation (DOR) [1] and dynamic angle spinning (DAS) [2]. Recently, it has been demonstrated that the line narrowing of the central transition can be conveniently obtained with a fixed rotor, as long as the motion of the rotation axis in space is replaced by changing the coherence state of the observed spins [4]. This experiment, referred to as multiple-quantum magic angle spinning (MQMAS), is technically straightforward and offers an attractive new method for the studies of a variety of materials, including catalysts [5–9]. A detailed description of this technique and of experimental strategies aimed at increasing its efficiency and quantitative accuracy has recently been published [10,11].

The development of new high-resolution methods in NMR inevitably leads to new possibilities of measuring the interactions between the nuclei under study and the neighboring spins. Several methods that measure the connectivities between half-integer quadrupolar nuclei (S) and their spin-$\frac{1}{2}$ neighbors (I) under high-resolution were recently developed. Most of these methods utilize indirect excitation via cross

*Corresponding author.

0920-5861/99/$ – see front matter © 1999 Elsevier Science B.V. All rights reserved.
PII: S0920-5861(98)00445-3

polarization (CP) for spectral editing of the DOR [12] and MQMAS [13,14] spectra or for the DAS- [15] and MQMAS-based [16] heteronuclear correlation (HETCOR) experiments. Although these techniques provide a new means of analyzing the intermediate range ordering in various inorganic solids, they suffer from the quantitative uncertainties that are associated with the complex dynamics of polarization transfer. Demonstration of internuclear connectivities between spin-$\frac{1}{2}$ and quadrupolar nuclei can also be made by reintroducing the heteronuclear dipolar dephasing between these spins using rotor-synchronized RF pulses. A number of MAS-based methods for measurement of dipolar interactions were reported in the last decade, including rotational echo double resonance (REDOR) [17,18], transferred echo double resonance (TEDOR) [18,19], transfer of populations in double resonance (TRAPDOR) [20,21], rotational echo, adiabatic passage, double resonance (REAPDOR) [22] and dipolar exchange-assisted recoupling (DEAR) [23]. We have recently presented a method that combines MQMAS with (quadrupolar spin)-observe, (spin-$\frac{1}{2}$)-dephase REDOR [24]. This technique, which we referred to as MQ-t_2-REDOR, proved to be a promising new tool for spectral editing and, additionally, for studying the internuclear distances in complex systems involving quadrupolar spins under high-resolution conditions. The CP-MQMAS and MQ-t_2-REDOR methods were immediately put to test in the studies of catalytic materials in our laboratories. In this paper, we briefly review the CP-MQMAS and MQ-t_2-REDOR methods and discuss their future applications. In addition, we present two new schemes for the MQ-based experiments, referred to as MQ-t_1-REDOR and MQMAS with dipolar dephasing (DD-MQMAS), in which the dipolar coupling between spins is reintroduced during the multiple- rather than single-quantum evolution.

2. MQMAS with cross polarization

The cross polarization experiment utilizes the dipolar coupling between two spins to produce nuclear magnetization of the observed spins via CP transfer. The standard spin-$\frac{1}{2} \rightarrow$ spin-$\frac{1}{2}$ CP experiments are usually performed between abundant and rare spins to enhance the nuclear magnetization of the latter [25]. The polarization transfer in such systems is well understood, and obtaining quantitative spectra is relatively easy. When appropriate line narrowing methods are applied to both spins, this polarization can be further employed to obtain high-resolution HETCOR spectra. Such experiments are routinely used to probe the proximity of different spin-$\frac{1}{2}$ nuclei in solids [26].

For reasons to be discussed later, the cross polarization between spin-$\frac{1}{2}$ and quadrupolar nuclei often performs poorly and does not lead to enhanced sensitivity. However, it remains a very useful method to study the correlations between dipolar-coupled nuclei. The first high-resolution HETCOR NMR spectroscopy involving quadrupolar nuclei used DAS to average the second-order quadrupolar interaction [15]. The development of MQMAS spectroscopy was followed by attempts to couple this method with CP, as well. In principle, this experiment can use either the spin-$\frac{1}{2}$ nuclei as the original source of magnetization (I $\rightarrow$ S), or can be done in reverse (S $\rightarrow$ I). The pulse sequences and coherence transfer pathways used in the first implementations of these techniques are shown in Fig. 1.

In the experiment shown in Fig. 1(a), the I $\rightarrow$ S polarization transfer is followed by the standard *z*-filtered MQMAS scheme [13,14]. We have shown that this CP-MQMAS experiment is possible between ^{19}F and ^{27}Al nuclei in fluorinated triclinic chabazite-like $AlPO_4$ aluminophosphate [13]. The crystal structure of this compound contains three equally populated aluminum sites: an Al_1 site octahedrally coordinated to four oxygen and two fluorine atoms, and two tetrahedral sites labeled Al_2 and Al_3. The MQMAS spectrum of Fig. 2(a) shows these three resonances are well resolved. We note that distinction between the tetrahedral sites could not be made with MAS only (also see Fig. 6(a)). The aluminum site that is bonded to fluorine was easily distinguished in the CP-MQMAS spectrum (Fig. 2(b)), which demonstrated the utility of this method for spectral editing.

A similar experiment was applied for probing the interaction of ^{1}H nuclei in water with the framework aluminum of fully rehydrated $AlPO_4$-11 aluminophosphate [14]. As Fig. 3 demonstrates, ^{1}H$\rightarrow^{27}$Al CP-MQMAS allowed for distinguishing the Al sites that are most and least susceptible to hydration. Such distinction would not be possible without the separation of ^{27}Al resonances under high-resolution condi-

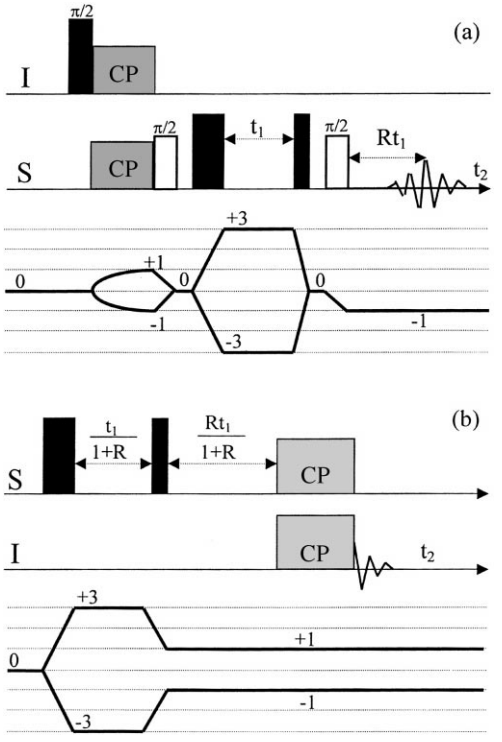

Fig. 1. Pulse sequences and coherence transfer pathways for I → S (a) and S → I (b) CP-3MQMAS methods. The conditions and phase cycling schemes used in these experiments are detailed in Ref. [13,14] and [16], respectively. The ratio *R* defines the time of formation of an isotropic echo in the t_2 domain [4].

tions. Although the same result was obtained earlier by Wu et al. using CP-DOR [27], the CP-3MQMAS method yielded a sideband-free, two-dimensional spectrum in comparable experimental time. Most recently, we used a combination of $^{19}F \rightarrow ^{27}Al$ and $^{1}H \rightarrow ^{27}Al$ CP-3QMAS techniques to study the structures of oxyfluorinated aluminophosphate $(NH_4)_{0.88}(H_3O)_{0.12}AlPO_4(OH)_{0.33}F_{0.67}$, referred to as CJ2 [28].

We note that the experimental scheme of Fig. 1(a) can be easily modified to achieve a 3D high-resolution HETCOR experiment by inserting an additional evolution period between the initial $(\pi/2)_I$ pulse and the CP transfer. However, due to unfavorable relaxation rates such as experiment would require a very long acquisition time. Therefore, it is advantageous for HETCOR NMR to use the 2D scheme shown in Fig. 1(b) [16], which utilizes the S → I polarization transfer from fast relaxing quadrupolar nuclei. Under MAS conditions, these experiments were performed earlier on catalytic systems [18,29,30] but, to the best of our knowledge, have not yet been applied to such systems under high-resolution. Fig. 4 displays the utility of such a technique on a sample of $Na_3P_3O_9$ [16].

The application of the above methods to half-integer quadrupolar nuclei is difficult due to the convoluted spin dynamics involved in both the spin locking and the CP processes under static and MAS condi-

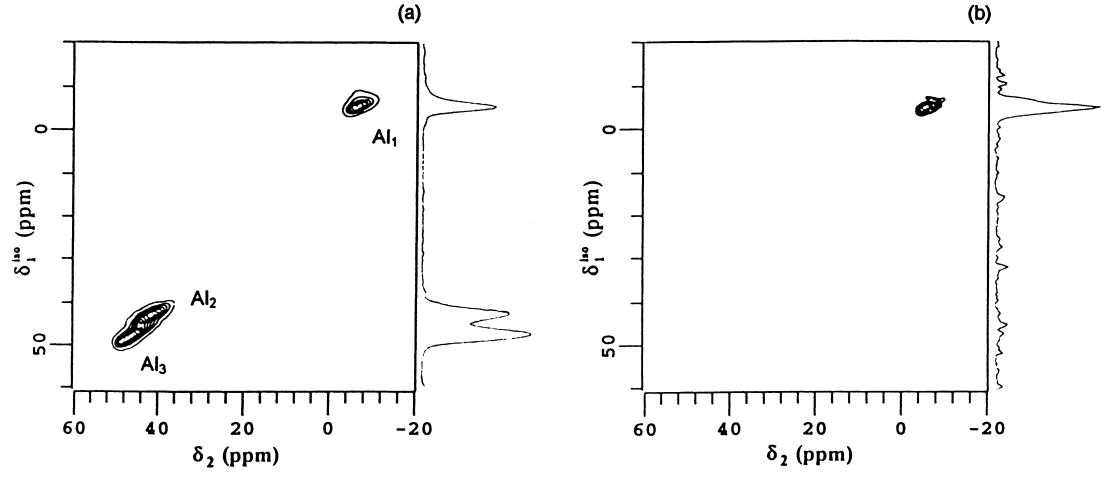

Fig. 2. 2D NMR spectra of ^{27}Al in $AlPO_4$-CHA obtained using 3QMAS (a) and ^{19}F–^{27}Al CP-3QMAS (b). The octahedral site Al_1 is directly coordinated to fluorine. The spectra were taken at 9.4 T on a Chemagnetics Infinity spectrometer using a 3.2 mm CPMAS probehead. The Hartman–Hahn condition was established with an RF field ν_{1S} of ∼5 kHz under a MAS speed of 20 kHz. ^{19}F decoupling was applied during evolution and acquisition times using ν_{1I} of ∼80 kHz. The phase cycling scheme is described in Ref. [14].

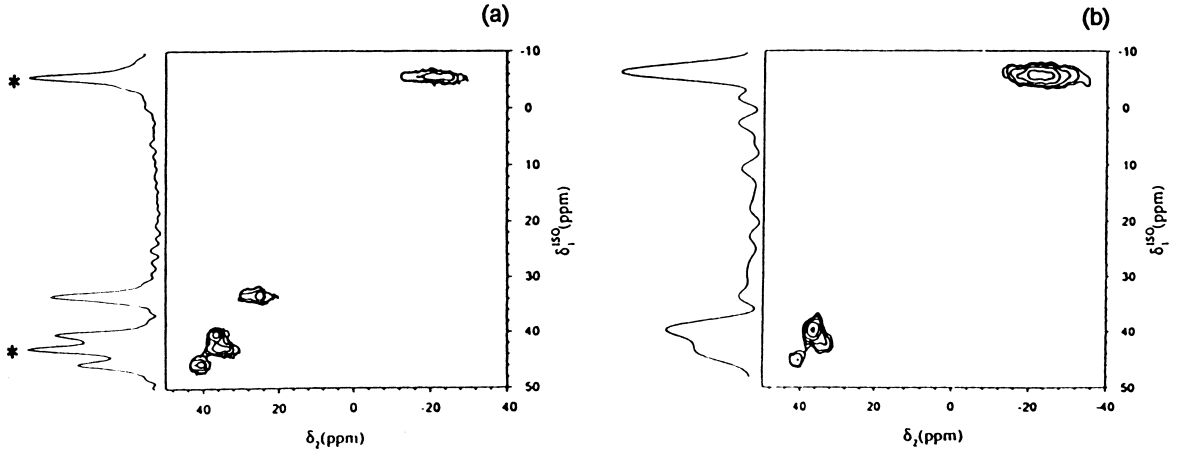

Fig. 3. 2D NMR spectra of ^{27}Al in $AlPO_4$-11 obtained using 3QMAS (a) and $^{1}H \rightarrow {}^{27}Al$ CP-3QMAS (b). The four- and six-coordinated Al species that exhibit the strongest interaction with adsorbed water are marked with asterisks in Fig. 3(a). The spectra were acquired with a Bruker ASX-400 spectrometer and a 4 mm CPMAS probehead. The experimental conditions were similar to those described in the caption of Fig. 2, except for the spinning speed, which was 12 kHz.

tions. These dynamics are strongly anisotropic with respect to crystallite orientation and depend on the relative size of the quadrupole frequency ν_Q, the amplitudes of the RF field applied to the I and S spins ν_{1I} and ν_{1S}, the spinning speed ν_r and the resonance offsets $\delta\nu_{0I}$ and $\delta\nu_{0S}$. Although significant progress has recently been made due to several excellent contributions (see, for example, Ref. [12,31–35]), the understanding of these processes remains incomplete. Some of the challenges involved in such experiments are briefly reviewed below.

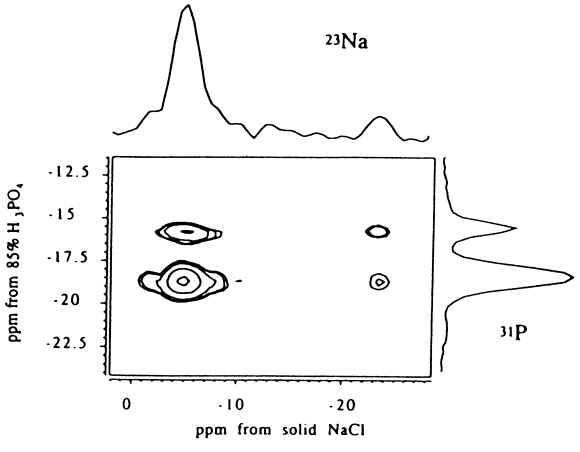

Fig. 4. 2D HETCOR NMR spectra of ^{23}Na and ^{31}P in $Na_3P_3O_9$ obtained using 3QMAS to produce an isotropic dimension for the S spins [16]. A similar spectrum was obtained earlier by Jarvie et al. using the 2D DAS-CPMAS experiment [15].

The Hartmann–Hahn matching condition for CP [36] requires that $\nu_{1I} = \nu_{nut}$, where ν_{nut} is the nutation frequency associated with the central transition of the S spin. In a simple case of on-resonance, static CP between spin-$\frac{1}{2}$ nuclei and the single quantum central transition coherence of quadrupolar nuclei this translates to [33]

$$\nu_{1I} = \nu_{1S}, \ |Q| \ll \nu_{1S} \tag{1}$$

and

$$\nu_{1I} = \left(S + \tfrac{1}{2}\right)\nu_{1S}, \ |Q| \gg \nu_{1S}, \tag{2}$$

where Q is the first-order quadrupole splitting

$$Q(\theta, \varphi) = \tfrac{1}{2}\nu_Q(3\cos^2\theta - 1 - \eta\sin^2\theta\cos 2\varphi) \tag{3}$$

with polar angles θ and φ relating the Zeeman field to the electric field gradient principal axis system, and η being the asymmetry parameter. The quadrupole frequency ν_Q is given by

$$\nu_Q = \frac{3C_Q}{2S(2S-1)h} \tag{4}$$

where the quadrupolar coupling constant C_Q is proportional to the nuclear quadrupole moment and the magnitude of the electric field gradient.

When CP of the 3Q transition of spin-$\frac{3}{2}$ nuclei is involved, the Hartmann–Hahn condition for a specific crystallite is [31]

$$\nu_{1I} = \frac{(2/3)\nu_{1S}^3}{[Q(\theta,\varphi)]^2}, \ |Q| \gg \nu_{1S} \quad (5)$$

where, again, the conditions $\nu_r = \delta\nu_{0I} = \delta\nu_{0S} = 0$ are assumed. Since $Q(\theta,\varphi)$ varies widely with the orientations of crystallites, the Hartmann–Hahn condition of Eq. (5) cannot be well defined in a polycrystalline sample.

MAS complicates both spin-locking [32] and polarization transfer [33] by making the quadrupole splitting $Q(\theta,\varphi)$ time dependent. The effect of MAS can be categorized based on the magnitude of the parameter $\alpha = \nu_{1S}^2/\nu_Q\nu_r$ that is related to the speed with which $Q(\theta,\varphi)$ crosses zero during sample spinning [32]. It has been shown that efficient spin-locking can be maintained when $\alpha \ll 1$ (sudden passage) or when $\alpha \gg 1$ (adiabatic passage), whereas the intermediate case $\alpha \cong 1$ results in a loss of the spin-locked state. In addition, a periodic modulation of the I–S dipolar interaction has profound effect on the CP process itself [33,37]. In the simple case of $|Q| \gg \nu_{1S}$ and $\delta\nu_{0I} = \delta\nu_{0S} = 0$, the Hartmann–Hahn matching condition is

$$\nu_{1I} = \pm\left(S + \tfrac{1}{2}\right)\nu_{1S} \pm n\nu_r, \ n = 1, 2, \ldots \quad (6)$$

The sudden regime ($\alpha \ll 1$) implies the use of low RF fields, which, in turn, can drastically influence the spin locking and CP transfer efficiency for different spins due to the convoluted interplay between ν_{1S}, ν_{1I}, ν_r and the resonance offsets $\delta\nu_{0S}$ and $\delta\nu_{0I}$ [12,34]. The optimization of the Hartmann–Hahn match becomes very ambiguous in this regime. As a result, the absence of a resonance in the CP spectrum should not be used as evidence for the lack of I $\leftrightarrow$ S connectivity without some careful experimentation. Also, in the case of I $\rightarrow$ S CPMAS experiments with low RF fields, the polarization is transferred exclusively to the $\pm$1Q central transition coherence of the S spins.

The spin dynamics under conditions where adiabatic passages occur ($\alpha \gg 1$) is also complex. Experimentally, the $\alpha \gg 1$ regime can be approached by reducing the spinning speed and/or increasing the RF power. However, since MQMAS requires the use of highest available ν_r [38,39], we consider only the latter option. Under typical conditions of $\nu_r \geq 10$ kHz and $\nu_Q = 1$ MHz, this translates to ν_{1S} being much greater than 100 kHz. In this case, the condition of $|Q| \gg \nu_{1S}$ is no longer satisfied for most of the crystallites and the nutation behavior of the S spins varies strongly with changing orientation. Consequently, no simple Hartmann–Hahn formulae can be derived for 1Q and MQ CP transfer in the range $|Q| \cong \nu_{1S}$ [31,33], and numerical simulations of the spin density matrix

Table 1
Optimized intensities, RF fields ν_{1S} and contact times τ_{CP} obtained via direct CP of 1Q and 3Q coherences using $\nu_{1I} = 200$ kHz

S	C_Q	Coherence	ν_D (kHz)											
			10			5			2			1		
			Intensity	ν_{1S} (kHz)	τ_{CP} (μs)	Intensity	ν_{1S} (kHz)	τ_{CP} (μs)	Intensity	ν_{1S} (kHz)	τ_{CP} (μs)	Intensity	ν_{1S} (kHz)	τ_{CP} (μs)
$\frac{3}{2}$	1.6	1Q	0.84	120	190	0.34	120	250	0.10	120	1150	0.03	120	2300
		3Q	0.86	120	190	0.36	120	250	0.12	120	1150	0.04	120	2300
	3.2	1Q	0.31	80	150	0.10	80	170	0.03	110	950	0.01	110	2100
		3Q	0.30	110	220	0.10	110	220	0.08	110	1100	0.03	110	2300
$\frac{5}{2}$	3.27	1Q	0.42	170	150	0.40	185	150	0.17	185	630	0.10	185	720
		3Q	0.45	170	110	0.44	185	150	0.17	185	630	0.10	185	720
	6.53	1Q	0.22	70	130	0.09	75	290	0.02	75	510	0.02	75	1760
		3Q	0.22	70	140	0.06	75	310	0.02	75	510	0.02	165	1760

Other parameters used in simulations were as follows: the Larmor frequencies $\nu_{0I} = 4\nu_{0S} = 400$ MHz, $\delta\nu_{0I} = \delta\nu_{0S} = 0$, $\nu_r = 20$ kHz, while ν_{1S} was allowed to vary between 5 and 200 kHz. The C_Q values have been adjusted to give the same spectral-widths for spins $\frac{3}{2}$ and $\frac{5}{2}$. For each pair of C_Q and ν_D values, ν_{1S} and τ_{CP} were varied independently in order to obtain the maximum efficiency of the CP transfer to 1Q coherence. The same optimization was repeated for the 3Q coherence. The efficiencies are normalized to the maximum intensity that can be observed on the central-transition after a selective 90° pulse.

evolution are needed to unravel the complex behavior of spins during spin locking and CP under these conditions. We performed such simulations using a home-made program, PULSAR [40]. As can be expected, the simulations show that the CP transfer is less affected by the interference from ν_r, $\delta\nu_{0S}$ and $\delta\nu_{0S}$. Unfortunately, it is also less efficient than in case of the weak RF fields, except for samples with low values of C_Q and large dipolar couplings.

Some of the results obtained with $\nu_r = 20$ kHz are summarized in Table 1, which shows the optimized 1Q and 3Q intensities obtained by cross-polarization of spins $S = \frac{3}{2}$ and $\frac{5}{2}$ using $\nu_{1I} = 200$ kHz. Clearly, the optimized contact times strongly depend on C_Q and ν_D. Although the efficiency of direct CP excitation of MQ coherences rapidly declines for large values of C_Q and small dipolar coupling ν_D, the data of Table 1 show that such excitation is feasible in the adiabatic regime. Also, there is a striking similarity between the 1Q and 3Q intensities obtained with each set of C_Q and ν_D values. Most likely, this equilibration of coherences occurs via RIACT-like (rotation-induced adiabatic coherence transfer) mechanism [32,41], which generates fast $1Q \leftrightarrow 3Q$ transfers in cross-polarized nuclei. While our experimental efforts failed in achieving direct cross polarization to 3Q, such CP between $^1H \rightarrow ^{23}Na$ has recently been observed by others in a sample of CH_3CO_2Na [42,43].

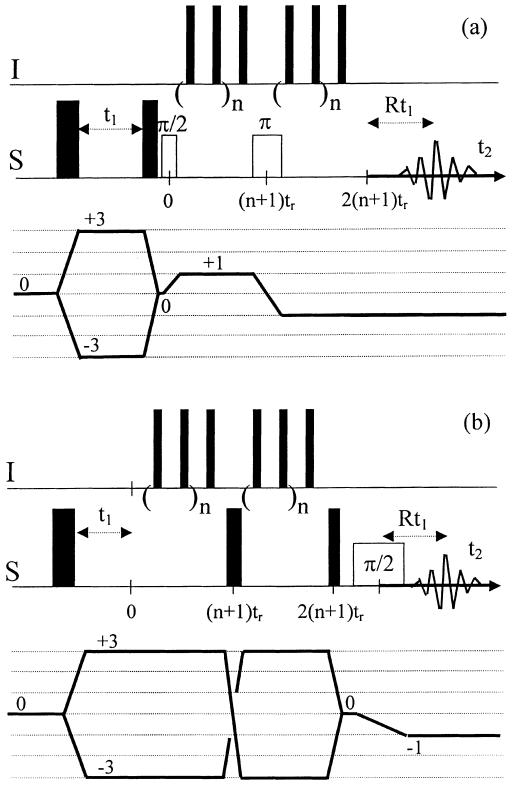

Fig. 5. Pulse sequences used in the 3Q-t_2-REDOR (a) and 3Q-t_1-REDOR (b) experiments. In these figures, n is an integer number and t_r denotes the rotor period.

3. MQMAS with dipolar recoupling via REDOR

The quantitative uncertainties that are associated with CP transfer can be circumvented by combining the high-resolution capabilities of MQMAS with the direct determination of hetero-nuclear dipolar couplings via REDOR. Fig. 5 shows the schematic diagrams of two MQ-REDOR experiments, referred to as MQ-t_1-REDOR and MQ-t_2-REDOR. MQ-t_2-REDOR (Fig. 5(a)) employs dipolar recoupling between spins I and S using a series of π pulses that are applied to the I spins during single quantum evolution. In the second method (Fig. 5(b)), the π pulses are shifted into the MQ evolution.

The MQ-t_2-REDOR technique, described in detail elsewhere [24], employs two strong and two selective RF pulses at the Larmor frequency ν_{0S} with phases cycled to select the $0 \rightarrow \pm p \rightarrow 0 \rightarrow +1 \rightarrow -1$ coherence pathway [44]. When spaced by an integer number of rotor periods the selective pulses create two windows in which the sequences of π pulses can be applied to the spin-$\frac{1}{2}$ nuclei. Similar to the standard REDOR experiment [17], the role of the π pulses is to prevent MAS from refocusing the dephasing due to the dipolar interaction between spins I and S.

We have demonstrated the spectral editing capabilities of the MQ-t_2-REDOR method [24] using the same $AlPO_4$-CHA sample that was previously examined via CP-MQMAS (see Fig. 2). The so-called REDOR difference, obtained by subtracting the MQMAS spectra obtained without and with the dephasing pulses is shown in Fig. 6(c)–(d). As expected, only the resonance from fluorinated site (Al_1) remains in the spectrum of Fig. 6(c). However, the capabilities of this method extend beyond the spectral editing. By changing the number of rotor cycles, we were able to measure the so-called REDOR

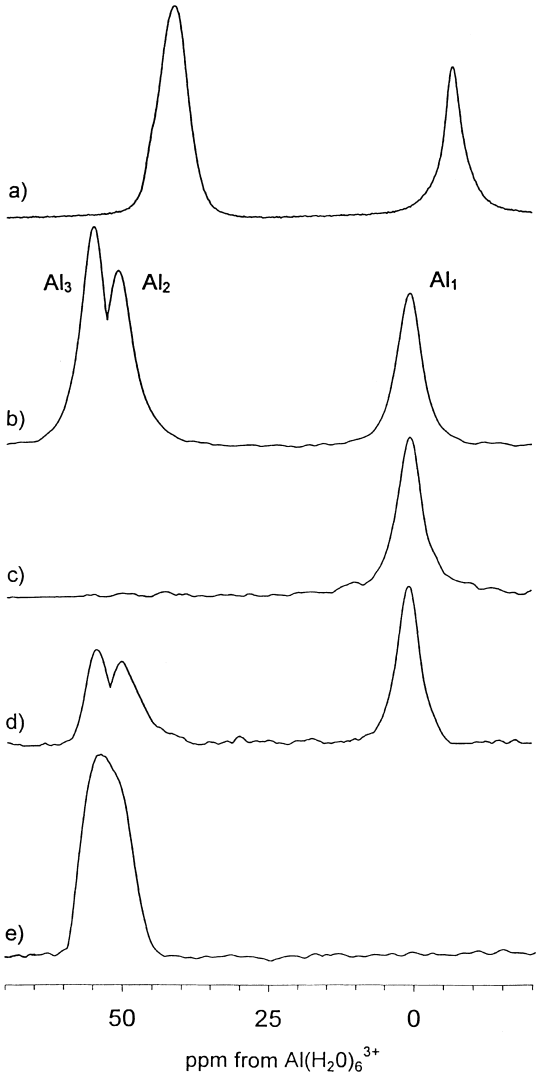

Fig. 6. ^{27}Al NMR spectra of fluorinated $AlPO_4$-CHA aluminophosphate: (a) MAS; (b) 3QMAS; (c) 3Q-t_2-REDOR difference for $n = 1$; (d) 3Q-t_2-REDOR difference $n = 29$; DD-MQMAS (e). In figures (b)–(e), only the isotropic projections of sheared 2D spectra are shown. The spectra were acquired at 9.4 T using a Chemagnetics 3.2 mm MAS probehead and a MAS speed of 20 kHz. The selective $\pi/2$ and π pulses for the S spins were applied using an RF field of ~10 kHz; the remaining pulses for both S (^{27}Al) and I (^{19}F) spins used an RF field of ~300 kHz.

curves [17] for the various Al species and estimate their distances from the nearest fluorine. The obtained results, $r_{Al_1-F} = 1.88(\pm 0.02)$ Å, $r_{Al_2-F} = 4.1(\pm 0.2)$ Å and $r_{Al_3-F} = 4.7(\pm 0.2)$ Å are in good agreement with the synchrotron radiation data (1.88, 3.94 and 5.72 Å, respectively [45]), in spite of the fact that the NMR estimates were made using the standard method for an isolated I–S spin pair and, in addition, neglected the effect which the anisotropy of MQ excitation with respect to crystallite orientation may have on the REDOR curve. We note that for the Al_1 site, the resolution is sufficient to permit the REDOR measurement without including the MQMAS method, however, since tetrahedral aluminums Al_2 and Al_3 are not resolved by MAS alone (see Fig. 6(a)), and the standard 1Q-REDOR experiment yields only a combined REDOR curve for these sites. The above data allowed, for the first time, the assignment of the resonances at 43.9 and 47.6 ppm to Al_2 and Al_3, respectively.

Most recently, we proposed the MQ-t_1-REDOR experiment (see Fig. 5(b)), which employs the REDOR sequence during multiple rather than single quantum evolution [46]. Because the dipolar effect is enhanced by a factor of p during the p-quantum evolution, this technique has potential for improved sensitivity toward weak dipolar interactions. Indeed, our results showed that for all aluminum sites in $AlPO_4$-CHA the apparent size of ^{19}F–^{27}Al coupling measured using 3Q-t_1-REDOR was higher by a factor of 3 when compared with the data obtained with 3Q-t_2-REDOR. A more detailed description of this new experiment is currently being prepared as a separate publication.

We note, however, that the measurement of REDOR curve by the MQ-t_1-REDOR technique requires more experimental time than the MQ-t_2-REDOR method because of the significant changes of the coherence levels ($|\Delta p| = 2p$) involved in the $0 \rightarrow \pm p \rightarrow \mp p \rightarrow 0 \rightarrow -1$ coherence transfer pathway. Fig. 7

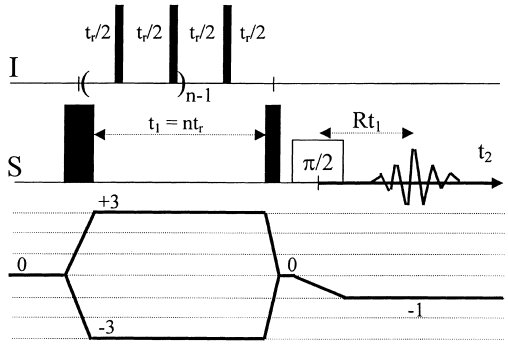

Fig. 7. Pulse sequence used in the DD-MQMAS experiment.

shows an easier method that uses the standard z-filtered MQMAS scheme for spins S, while the dipolar recoupling with spins I is accomplished using a series of π pulses applied synchronously with the rotor frequency to the I spins. We refer to this experiment as MQMAS with dipolar dephasing (DD-MQMAS). The simpler $0 \rightarrow \pm p \rightarrow 0 \rightarrow -1$ coherence pathway that is used here results in line broadening, but allows for fast, yet only qualitative, determination of the internuclear connectivities in well crystallized compounds. Again, the same $AlPO_4$-CHA sample was used to test this method (see Fig. 6(e)). As already demonstrated in Fig. 2(a) and Fig. 6(b), the isotropic MQMAS spectrum shows three resonances with residual linewidths mainly due to a small distribution of local surroundings. The Al_1 site resonance is broadened beyond observation in the spectrum of Fig. 6(e), and thus the connectivity between this site and fluorine is clearly demonstrated. As expected, dipolar recoupling affects the isotropic linewidths of the remaining two sites, as well.

4. Conclusions

The capabilities of MQMAS can be extended by combining it with cross polarization and with REDOR. The advantage of these techniques is that they provide direct inference of the connectivities between spin-$\frac{1}{2}$ (e.g. ^{1}H, ^{19}F, ^{31}P) and quadrupolar (e.g. ^{11}B, ^{17}O, ^{23}Na, ^{27}Al) nuclei in solids in the isotropic spectra of quadrupolar nuclei, i.e. without the limitations in resolution imposed by MAS. Additionally, the MQ-REDOR methods yielded the internuclear distances in these systems. We have demonstrated the strength of these techniques in the studies of ^{1}H–^{27}Al and ^{19}F–^{27}Al spin pairs in aluminophosphate molecular sieves. Further applications will include determination of the arrangement of molecules and atoms in adsorbent/adsorbate systems.

Acknowledgements

This research was supported at Ames Laboratory by the U.S. Department of Energy, Office of Basic Energy Sciences, Division of Chemical Sciences, under Contract W-7405-Eng-82 and at the University of Lille by the Region Nord-Pas de Calais. The authors thank Drs. P.J. Grandinetti, C.P. Grey and D. Massiot for valuable discussions.

References

[1] A. Samoson, E. Lippmaa, A. Pines, Mol. Phys. 65 (1988) 1013.
[2] K.T. Mueller, B.Q. Sun, G.C. Chingas, J.W. Zwanziger, T. Terao, A. Pines, J. Magn. Reson. 86 (1990) 470.
[3] J.-P. Amoureux, Solid State Nucl. Magn. Reson. 2 (1993) 83.
[4] L. Frydman, J.S. Harwood, J. Am. Chem. Soc. 117 (1995) 5367.
[5] J. Rocha, A.P. Esculcas, C. Fernandez, J.-P. Amoureux, J. Phys. Chem. 100 (1996) 17889.
[6] J. Rocha, Z. Lin, C. Fernandez, J.-P. Amoureux, Chem. Commun. (1996) 2513.
[7] P. Sarv, C. Fernandez, J.-P. Amoureux, K. Keskinen, J. Phys. Chem. 100 (1996) 19223.
[8] S. Ganapathy, T. Das, R. Vetrivel, L. Delevoye, C. Fernandez, J.-P. Amoureux, J. Am. Chem. Soc. 120 (1998) 4752.
[9] J.-P. Amoureux, F. Bauer, H. Ernst, C. Fernandez, D. Freude, D. Michel, U.-T. Pingel, Chem. Phys. Lett. 285 (1998) 10.
[10] A. Medek, J.S. Harwood, L. Frydman, J. Am. Chem. Soc. 117 (1995) 12779.
[11] J.-P. Amoureux, C. Fernandez, Solid State Nucl. Magn. Reson. 10 (1998) 211.
[12] W. Sun, J.T. Stephen, L.D. Porter, Y. Wu, J. Magn. Reson. A 116 (1995) 181.
[13] M. Pruski, D.P. Lang, C. Fernandez, J.-P. Amoureux, Solid State Nucl. Magn. Reson. 7 (1997) 327.
[14] C. Fernandez, L. Delevoye, J.-P. Amoureux, D.P. Lang, M. Pruski, J. Am. Chem. Soc. 119 (1997) 6858.
[15] T.P. Jarvie, R.M. Wenslow, K.T. Mueller, J. Am. Chem. Soc. 117 (1995) 570.
[16] S.H. Wang, S.M. De Paul, L.M. Bull, J. Magn. Reson. 125 (1997) 364.
[17] T. Guillion, J. Schaefer, J. Magn. Reson. 81 (1989) 196.
[18] C.A. Fyfe, K.T. Mueller, H. Grodney, K.C. Wong-Moon, Chem. Phys. Lett. 199 (1992) 198.
[19] A.W. Hing, S. Vega, J. Schaefer, J. Magn. Reson. 96 (1992) 205.
[20] E.R.H. van Eck, R. Jansen, W.E.J.R. Maas, W.S. Veeman, Chem. Phys. Lett. 174 (1990) 428.
[21] C.P. Grey, A.J. Vega, J. Am. Chem. Soc. 117 (1995) 8232.
[22] T. Guillion, Chem. Phys. Lett. 246 (1995) 325.
[23] J.R. Sachleben, V. Frydman, L. Frydman, J. Am. Chem. Soc. 118 (1996) 9786.
[24] C. Fernandez, D.P. Lang, J.-P. Amoureux, M. Pruski, J. Am. Chem. Soc. 120 (1998) 2672.
[25] A. Pines, M.G. Gibby, J.S. Waugh, J. Chem. Phys. 59 (1973) 569.
[26] D.P. Burum, A. Bielecki, J. Magn. Reson. 94 (1991) 645.
[27] Y. Wu, D. Lewis, J.S. Frye, A.R. Palmer, R.A. Wind, J. Magn. Reson. 100 (1993) 425.

[28] D.P. Lang, A. Bailly, M. Pruski, J.-P. Amoureux, C. Huguenard, M. Haouas, C. Gerardin, F. Taulelle, T. Loiseau, G. Ferey, in preparation.
[29] C.A. Fyfe, K.T. Mueller, H. Grodney, K.C. Wong-Moon, J. Phys. Chem. 97 (1993) 13484.
[30] C.A. Fyfe, K.C. Wong-Moon, Y. Huang, H. Grodney, K.T. Mueller, J. Phys. Chem. 99 (1995) 8707.
[31] S. Vega, Phys. Rev. A 23 (1981) 3152.
[32] A.J. Vega, J. Magn. Reson. 96 (1992) 50.
[33] A.J. Vega, J. Solid State Nucl. Magn. Reson. 1 (1992) 17.
[34] S.M. De Paul, M. Ernst, J.S. Shore, J.F. Stebbins, A. Pines, J. Phys. Chem. B 101 (1997) 3240.
[35] M.A. Eastman, in: 39th Experimental Nuclear Magnetic Resonance Conf., Poster M/TP 26, Pacific Grove, California, March, 1998.
[36] S.R. Hartmann, E.L. Hahn, Phys. Rev. 128 (1962) 2042.
[37] E.O. Stjeskal, J. Schaefer, J. Waugh, J. Magn. Reson. 28 (1977) 105.
[38] L. Marinelli, L. Frydman, Chem. Phys. Lett. 275 (1997) 188.
[39] J.-P. Amoureux, M. Pruski, D.P. Lang, C. Fernandez, J. Magn. Reson. 131 (1998) 170.
[40] J.-P. Amoureux, C. Fernandez, Y. Dumazy, J. Chim. Phys. 2 (1995) 1939.
[41] G. Wu, D. Rovnyak, R.G. Griffin, J. Am. Chem. Soc. 118 (1996) 9326.
[42] D. Rovnyak, M. Baldus, R.G. Griffin, in: 39th Experimental Nuclear Magnetic Resonance Conf., Poster W/Th 17, Pacific Grove, California, March, 1998.
[43] S.E. Ashbrook, S.P. Brown, S. Wimperis, in: 39th Experimental Nuclear Magnetic Resonance Conf., Poster W/Th 27, Pacific Grove, California, March, 1998.
[44] R.R. Ernst, G. Bodenhausen, A. Wokaun, Principles of Nuclear Magnetic Resonance in One and Two Dimensions, Oxford University Press, New York, 1987.
[45] M.M. Harding, B.M. Kariuki, Acta Crystallogr. C 50 (1994) 852.
[46] M. Pruski, C. Fernandez, D.P. Lang, A. Bailly, J.-P. Amoureux, in: 40th Rocky Mountain Conf., Poster 302, Denver, Colorado, July, 1998.